AMPLITUDE-DRIVEN-ADAPTIVE-NEIGHBORHOOD FILTERING OF HIGH-RESOLUTION POL-INSAR INFORMATION

Gabriel VASILE[(1)], Emmanuel TROUVÉ[(1)], Michel GAY[(2)] and Jean-Marie NICOLAS[(3)]

[(1)]: *Laboratoire d'Informatique, Systèmes, Traitement de l'Information et de la Connaissance*
Université de Savoie - ESIA - BP 806 - 74016 Annecy Cedex - FRANCE
Tel: +33 450 096 548 - Fax: +33 450 096 559 - Email: {gabriel.vasile|emmanuel.trouve}@univ-savoie.fr

[(2)]: *Laboratoire des Images et des Signaux - BP 46, F-38402 - 38402 Saint-Martin-d'Hres - FRANCE*
Tel: +33 476 826 260 - Fax: +33 476 826 384 - Email: michel.gay@lis.inpg.fr

[(3)]: *GET Télécom Paris - 46, Rue Barrault - 75634 Paris Cedex 13 - FRANCE*
Tel: +33 145 818 129 - Fax: +33 145 813 794 - Email: nicolas@tsi.enst.fr

ABSTRACT

In this paper a new method for filtering coherency matrices issued from Synthetic Aperture Radar (SAR) polarimetric interferometric data is presented. For each pixel of the interferogram, an adaptive neighborhood is determined by a region growing technique driven exclusively by the amplitude image information [1], [2]. All the available amplitude images of the interferometric couple are fused in the region growing process to ensure the stationarity hypothesis of the derived statistical population.

In addition, for preserving local stationarity requirement of the interferogram, a phase compensation step is performed. Afterwards, all the pixels within the obtained adaptive neighborhood are complex averaged to yield the filtered values of the polarimetric and interferometric coherency matrices.

The method has been tested on airborne high-resolution polarimetric interferometric SAR images (Oberpfaffenhofen area - German Space Agency). For comparison purposes, the standard phase–compensated fixed multi–look filter and the linear adaptive coherence filter proposed by *Lee at al.* [3] were also implemented. Both subjective and objective performance analysis, including coherence edge detection, ROC graph and bias reduction tables, recommends the proposed algorithm as a powerful post-processing POL-InSAR tool.

1 Introduction

The SAR system measures both amplitude and phase of the backscattered signal, the result being one complex (Single Look Complex) image for each recording. The principle of SAR interferometry (In–SAR) relies on the acquisition of two such complex images under slightly different viewing angles. After the two initial images are coregistered, the normalized complex cross-correlation is computed. The most commonly known measures in interferometry are its magnitude, namely the *coherence*, and its *phase*. The coherence is usually used for describing the temporal stability of the acquired signal. The phase includes a geometrical component directly linked to the distance between the target and the sensor, providing information about the altitude of the target.

In order to estimate the coherence, the ensemble averages required by its definition are replaced by spatial averages: a number of L neighboring pixels are averaged to yield an estimate of the coherence and phase image (operation called "complex multilooking"). However, despite this initial estimation, both coherence and phase images are highly corrupted by noise. Hence, the need to improve coherence estimation arises in order to reduce the estimation bias and variance [4]. The use of larger window sizes with fixed shapes gives poor results, since the stationarity hypothesis is often no longer valid and the final resolution decreases.

Polarimetric synthetic aperture radar (POLSAR) is an extension of the SAR imaging system, the sensors being able to emit and receive two polarizations, usually horizontal (H) and vertical (V). Four polarization

configurations, usually denoted by HH, VV, HV and VH (according to the emitted and received polarization) are simultaneously available. Under the assumption of reciprocal symmetric backscattering, the HV and VH modes are fused and the resulting configuration is denoted by XX. Polarimetric acquisitions are characterized by the 3×3 polarimetric coherency matrix.

Interferometry in POLSAR (POL–InSAR) performs two acquisitions (spatially separated by the baseline) of the scattering matrix for each resolution cell. The advantages of interferometry (hight and/or movement information) are enhanced by the polarimetric decomposition techniques.

In order to estimate the normalized complex cross-correlation for obtaining the coherencies and the polarimetric interferometric covariance, the L neighboring pixels are averaged to yield an estimate of the correlation. However, despite this initial estimation, the results are highly corrupted by noise (speckle). A filtering step is very often required to finally obtain reliable estimates. Moreover, the high resolution of newly available SAR airborne images offers the opportunity to observe much thinner spatial features than the decametric resolution of the uptonow available satellite SAR images. Being able to preserve such a high resolution in robust estimations of POL-InSAR coherences is an important issue to make this information useful.

Different filtering strategies have been proposed over the last few years. The most commonly used filter is a polarimetric extension of the Boxcar Filter (BF), implemented for instance in $DIAPASON$© software developed by CNES (Centre National d'Etudes Spatiales). It computes the normalized complex cross-correlation for each pixel in a fixed–size centered neighborhood. This filter is used as a reference for comparing the results of newer filtering algorithms in many papers [1, 2, 3, 4]. However, the BF has the drawback (common to all of the non–adaptive filtering methods) that it cannot make the difference between noise and useful signal, and induces a blurring effect which increases with the achieved noise reduction.

In the framework of POL–InSAR imagery, *Lee et al.* proposed a spatially adaptive filtering method for improving the accuracy of the coherence estimation [3] . Eight directional sub–windows are defined in order to locate the most homogeneous area inside the considered neighborhood. The sub–window selection procedure is driven by the average of the six available span images of the interferometric pair. The pixels within the selected sub–window yield the filtered covariance matrix, which is derived from the locally linear minimum mean–squared error estimator of the 6x6 covariance matrix.

In this paper a new estimation technique of the coherency matrices issued from SAR polarimetric interferometric data is presented. Each pixel, an adaptive neighborhood is built by a region growing technique driven exclusively by the amplitude image information [1], [2]. All the available amplitude images of the interferometric couple are fused in the region growing process to ensure the stationarity hypothesis of the derived statistical population. The results of the method have been validated on L–Band E–SAR polarimetric interferometric data.

2 Polarimetric SAR images

The POL–InSAR data is obtained by two parallel passes separated by a baseline for interferometry. Most commonly they are collected in antenna scattering matrix form, for the pass $i \in \{1, 2\}$:

$$s_i = \begin{bmatrix} S_{HH_i} \\ \sqrt{2} S_{XX_i} \\ S_{VV_i} \end{bmatrix}. \tag{1}$$

By using the Pauli basis marices [5], the obtained coherent scattering vectors k_i are closer to the physical phenomena of wave scattering:

$$k_i = \frac{1}{\sqrt{2}} \begin{bmatrix} S_{HH_i} + S_{VV_i} \\ S_{HH_i} - S_{VV_i} \\ 2 S_{XX_i} \end{bmatrix}. \tag{2}$$

One complete representation of the data is the 6×6 Hermitian positive semidefinite covariance matrix:

$$C_{pol} = E\left\{ \begin{bmatrix} k_1 \\ k_2 \end{bmatrix} \begin{bmatrix} k_1^{*T} & k_2^{*T} \end{bmatrix} \right\} = \begin{bmatrix} T_{11} & \Omega_{12} \\ \Omega_{12}^{*T} & T_{22} \end{bmatrix}, \tag{3}$$

where $E\{...\}$ denotes the expectation value, T_{ii} are the 3x3 polarimetric coherency positive semidefinite Hermitian matrices from each pass, Ω_{12} being the interferometric polarimetric matrix between the polarized acquisitions:

$$T_{ii} = E\{k_i k_i^{*T}\} \quad and \quad \Omega_{12} = E\{k_1 k_2^{*T}\}. \tag{4}$$

The polarimetric covariance matrix can be also constructed from the original form from *Eq.1* but, being linearly related with the matrix C_{pol}, it can be easily obtained by a simple linear transform. For further interpretation of the scattering mechanisms, the matrix defined in *Eq.3* has been chosen in this paper.

3 Amplitude-Driven-Adaptive-Neighborhood (ADAN) Estimation

The initial estimates of the coherency matrices and the polarimetric interferometric covariance are obtained by regrouping L SLC pixels of the averaging window to form one pixel in the resulting images. However the obtained results are extremely noisy and a filtering step is required [1, 3].

The **A**daptive **N**eighborhoods (ANs) concept in image processing has been introduced by *Gordon at al.* in the framework of an application in medical imagery [6]. In each pixel (called *seed* when processed), a neighborhood of variable shape and dimensions is built by a region growing algorithm, containing only connected pixels that belong to the same statistical population as the seed. Only the values of pixels aggregated in the AN participate to the computation of the final value of the seed.

The main advantage of the method is stationarity preservation whilst a significant number of samples is gathered in the estimation window.

3.1 Amplitude Driven region growing

In the proposed method only the amplitude information is used to decide upon the pixel membership to the AN. Small homogenous regions within all six amplitude images correspond to ground areas with an homogenous cover which respect the stationarity hypothesis requirement for the estimation of the complex correlation in *Eq.3*.

The region growing is driven by all six amplitude images simultaneously. The initial complex multilooking provides a rough and noisy estimation of C_{pol} (6×6 matrix). A multivariate vector is built containing only the elements of the main diagonal of C_{pol}:

$$p(m,n) = \begin{bmatrix} [T_{11}]_{11}(m,n) & [T_{22}]_{11}(m,n) \\ [T_{11}]_{22}(m,n) & [T_{22}]_{22}(m,n) \\ [T_{11}]_{33}(m,n) & [T_{22}]_{33}(m,n) \end{bmatrix} = \begin{bmatrix} p_1(m,n) \\ p_2(m,n) \\ p_3(m,n) \end{bmatrix}. \tag{5}$$

Only the diagonal elements of the T_{ii} matrices have been chosen as they are real numbers and their estimation is more stable with respect to the speckle noise.

The algorithm for constructing the AN consists of four steps [2]:

1. ***Rough estimation of the seed value***.The marginal median in the 3x3 centered neighborhood is used as the seed value $\widehat{p}(m,n)$.
2. ***Region growing***. All the eight direct neighbors $p(k,l)$ of the seed are accepted inside the AN provided they meet the following aggregation test:

$$\sum_{i=1}^{3} \frac{\|p_i(k,l) - \widehat{p_i}(m,n)\|}{\|\widehat{p_i}(m,n)\|} \leq 3\frac{\sigma_n}{\mu_n}. \tag{6}$$

   where μ_n and σ_n are the speckle mean and standard deviation. The variation coefficient σ_n/μ_n is a standard parameter in SAR imagery, which is a constant known to be equal to $1/\sqrt{L_{eq}}$ (L_{eq} is the equivalent number of looks resulting from the initial averaging). Then, the same procedure is applied for all of the neighbors of the newly included pixels and so on. The region growing iterates in this manner until either the number of the pixels already included in the AN exceeds a predefined upper limit N_{max} or none of the neighbors verify the test condition given by *Eq. 6*. The pixels which have already been

tested but not accepted inside the AN (called *background pixels* in the sequel) are stored in a separate list.

3. ***Refined estimation of the seed value***. A more reliable estimator of the unspeckled seed value is now obtained by averaging the pixels included in this "strict" AN: $\overline{p}(m,n)$.

4. ***Reinspection of the background pixels***. The background pixels $p(o,p)$ of the list created in step 2 are tested again and aggregated in the AN provided that:

$$\sum_{i=1}^{3} \frac{\|p_i(o,p) - \overline{p_i}(m,n)\|}{\|\overline{p_i}(m,n)\|} \leq 6\frac{\sigma_n}{\mu_n}. \tag{7}$$

The test is less restrictive, as the inclusion threshold is twice as large as the one used in the first step of region growing.

3.2 Final estimation

The conventional filtering method performs a complex averaging over a fixed size sliding window estimating the master and slave coherency matrices and the polarimetric interferometric matrix from *Eq.3*. For the interferometric matrix Ω_{12} the geometrical component of the phase is removed to ensure phase stationarity within the neighborhood used for an "extended" complex multilooking. This component is derived from an estimation of 2D local frequencies as proposed in [7] . In this type of approach the number of pixels averaged may not be sufficient to reduce the estimation variance and the stationarity hypothesis is not always respected. The *AN* previously constructed solves these problems.

The proposed method recomputes the complex averaging over the largest possible neighborhood (without loosing stationarity). In the case of the Pol-InSAR data set, the matrix C_{pol} from *Eq.3* is estimated, by replacing the ensemble average required by its definition with a spatial average having as spatial support the AN driven by the six amplitude images (diagonal elements of the roughly estimated covariance matrix).

4 Results and discussion

The performances of the ADAN estimation method are analyzed using the data set acquired in 1999 by an airborne experimental E–SAR system. It targets Oberpfaffenhofen area from Wessling, Germany, representing a repeated pass interferometric fully polarimetric L-band (1.25 GHz) acquisition with a baseline of about 15 m.

After initial 2–look complex multilooking, the master (respectively slave) coherency matrix and the polarimetric interferometric covariance matrix are produced. Hence a direct interpretation of the matrix Ω_{12} is not relevant, the interferometric coherence and phase images are produced by taking its normalized absolute value and its argument. *Fig.1-(a),(d)* presents the absolute value of the initial master coherency matrix and the initial coherence map. Each result presented contains 3×3 images arranged in a matrix form. The order corresponds to the elements within the matrices T_{11} and Ω_{12} defined in *Eq.3*.

ADAN estimation is applied to the high-resolution data set. The results are presented and compared with those obtained by the Lee Adaptive Filter (LAF) [3] and the BF Filter [4]. The same phase slope compensation [7] is applied (in the estimation of the polarimetric interferometric matrix) for all three cases in order to evaluate the influence of the neighborhood only. The parameters used in the implementation of ADAN estimation are: $N_{max} = 50$ and $\sigma_n = 0.5$ (corresponding to 2–look images). *Fig.1-(c),(f)* presents the results obtained by ADANF estimation of the master coherency matrix and of the coherence maps corresponding to Ω_{12}. The BF filtering results are also presented in *Fig.1-(b),(e)*. One can observe that the ADAN estimation outperforms the FMF filter from a visual point of view: uniform areas are better smoothed, contours are better preserved, and bias is more reduced (*Fig.1*) .

In order to objectively assess the performances of results, the Receiver Operating Characteristics (ROC) and bias reduction tables were computed [1]. From the detection point of view, the LAF and the ADAN estimation have similar performances, both being better than the BF. The false alarm histogram shows better performances for the ADAN estimation.

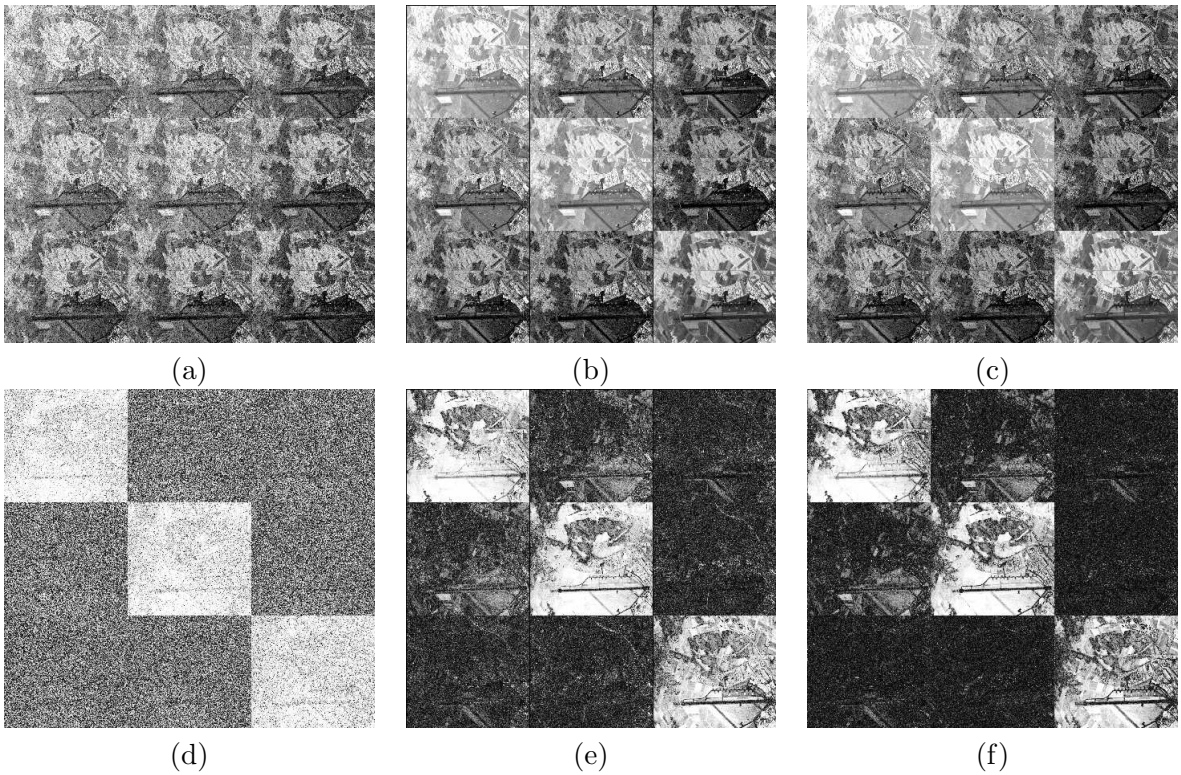

Figure 1: POL-InSAR data [$4620 \times 4221 \times 3$ pixels]: (a) original master coherency, (b) BF filtered master coherency, (c) ADAN estimated master coherency, (d) original coherence map, (e) BF filtered coherence, (f) ADAN estimated coherence.

Certain physical parameters of the scatterers can directly be estimated from POLSAR data. The information provided by SAR polarimetry allows the discrimination of different scattering mechanisms. One characteristic decomposition of coherency matrix for target scattering decomposition was proposed by Cloude and Pottiers in [8]. The target entropy and the $\alpha - \beta$ model assigne to each eigenvector of the coherency its corresponding coherent single scattering mechanism. Based on this decomposition, unsupervised classification for land applications was performed by *Lee at al.* by an iterative algorithm based on a complex Wishart density function [9]. *Fig.2* presents the results of the Wishart classification using as input images the master coherency either filtered by LAF or estimated by ADAN. As expected, due to the strong noise reduction on the homogenous area (fields, runway), the obtained results are much more regularized for the ADAN estimated coherency, whilst the thin structures (buildings) are very well delimited in both cases.

Cloude and Papathanassiou applied the polarimetric basis transformations in the POL–InSAR case and obtained interferograms between all possible linear combination of polarization states [10]. As polarization and interferometric coherence are tightly related, the optimization algorithm based on the maximization of the interferometric coherence was applied on the polarimetric interferometric ADAN estimated covariance matrix. One future goal is to inject this information into a fully POL-InSAR classification algorithm.

5 Conclusion

A new technique for filtering coherency matrices issued from an SAR polarimetric interferometric pair has been presented. The proposed method uses adaptive neighborhoods as spatial support, derived with respect to the amplitude information. All the available amplitude images of the interferometric couple are combined in the region growing procedure to ensure the stationarity of the averaging region. The proposed filter recomputes the polarimetric covariance matrix by averaging over the largest possible neighborhood.

The experimental results have proved that the noise is greatly reduced, the coherence bias is reduced, while the

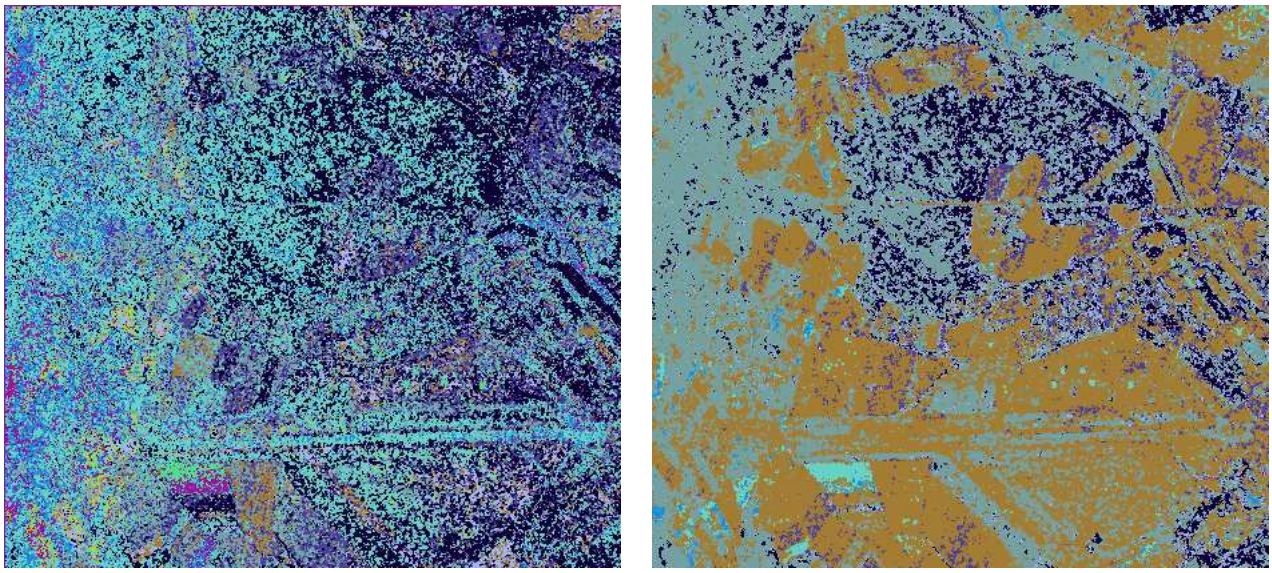

(a) (b)

Figure 2: POL-SAR Wishart classification data of the master coherency [4620×4221 pixels]: (a) LAF, (b) ADAN estimated.

contours and fine details are preserved and the blurring effect is avoided. Such approach allows the preservation of the high–resolution in computing polarimetric interferometric features, which provide useful information for further physical parameter extraction.

References

[1] G. Vasile, E. Trouvé, M. Ciuc, and V. Buzuloiu. General adaptive neighborhood technique for improving SAR interferometric coherence and phase estimation. *J. Opt. Soc. Am. A*, 21(8):1455–1464, august 2004.

[2] G. Vasile, E. Trouvé, M. Ciuc, P. Bolon, and V. Buzuloiu. Improving coherence estimation for high resolution polarimetric SAR interferometry. In *Geoscience and Remote Sensing Symposium, IGARSS '04, Anchorage, USA*, volume III, pages 1796–1799, 2004.

[3] J.S. Lee, S.R. Cloude, K. Papathanassiou, M.R. Grunes, and I.H. Woodhouse. Speckle filtering and coherence estimation of polarimetric SAR interferometry data for forest applications. *IEEE Transactions on Geoscience and Remote Sensing*, 41(10):2254–2263, 2003.

[4] R. Touzi, A. Lopes, J. Bruniquel, and P.W. Vachon. Coherence estimation for SAR imagery. *IEEE Transactions on Geoscience and Remote Sensing*, 37(1):135–149, 1999.

[5] S.R. Cloude and K.P. Papathanassiou. Polarimetric SAR interferometry. *IEEE Transactions on Geoscience and Remote Sensing*, 36(5):1551–1565, september 1998.

[6] R. Gordon and R.M. Rangayyan. Feature enhancement of film mammograms using fixed and adaptive neighborhoods. *Applied Optics*, 23(4):560–564, february 1984.

[7] E. Trouvé, M. Caramma, and H. Maître. Fringe detection in noisy complex interferograms. *Applied Optics*, 35(20):3799–3806, July 1996.

[8] S.R. Cloude and E. Pottier. A review of target decomposition theorems in radar polarimetry. *IEEE Transactions on Geoscience and Remote Sensing*, 34(2):498–518, march 1996.

[9] J.S. Lee, M.R. Grunes, T.L. Ainsworth, D. Li-Jen, D.L. Schuler, and S.R. Cloude. Unsupervised classification using polarimetric decomposition and the complex Wishart classifier. *IEEE Transactions on Geoscience and Remote Sensing*, 37(5):2249–2258, september 1999.

[10] K.P. Papathanassiou, A. Reigber, R. Scheiber, R. Horn, A. Moreira, and S.R. Cloude. Airborne polarimetric SAR interferometry. In *Geoscience and Remote Sensing Symposium Proceedings, IGARSS '98, Seattle, USA*, volume IV, pages 1901–1903, 1998.